

Stochastic Modeling of Experimental Chaotic Time Series

Thomas Stemler,^{*} Johannes P. Werner, and Hartmut Benner

Institute for Solid State Physics, Darmstadt University of Technology, Hochschulstraße 6, D-64289 Darmstadt, Germany

Wolfram Just[†]

School of Mathematical Sciences, Queen Mary/University of London, Mile End Road, London E1 4NS, United Kingdom

(Received 21 August 2006; published 24 January 2007)

Methods developed recently to obtain stochastic models of low-dimensional chaotic systems are tested in electronic circuit experiments. We demonstrate that reliable drift and diffusion coefficients can be obtained even when no excessive time scale separation occurs. Crisis induced intermittent motion can be described in terms of a stochastic model showing tunneling which is dominated by state space dependent diffusion. Analytical solutions of the corresponding Fokker-Planck equation are in excellent agreement with experimental data.

DOI: [10.1103/PhysRevLett.98.044102](https://doi.org/10.1103/PhysRevLett.98.044102)

PACS numbers: 05.45.Tp, 05.10.Gg, 05.40.-a, 07.50.Ek

Introduction.—Modeling dynamical degrees of freedom by suitable stochastic forces is a classical subject in theoretical physics and applied mathematics. While the replacement of many degrees of freedom in a thermodynamic system by Gaussian white noise is a textbook example and the foundation of, e.g., irreversible thermodynamics [1] it is quite a recent finding that few chaotic degrees of freedom can be modeled by stochastic differential equations (cf., e.g., [2] for a seminal reference in the context of climate research, or [3,4] for a mathematical account). To some extent such approaches rely on the property that certain nice chaotic dynamical systems can be described rigorously in terms of Markov chains (cf., e.g., [5]). Meanwhile, the modeling of chaotic dynamics by suitable stochastic systems has been applied in diverse contexts, e.g., for the confirmation of stochastic models in hydrodynamics [6], analysis of stock market data [7], or for climate models [8].

Above all, in theoretical terms such approaches rely on time scale separation such that irrelevant fast chaotic degrees of freedom can be described in terms of a noise process acting on slow relevant degrees of freedom. While in mathematical models time scale separation can be usually achieved by introducing some small parameter the situation may be less obvious in real experimental contexts, in particular, when no established mathematical model is at hand like in nanoscience or biophysics. Nevertheless, even in these fields stochastic models seem to be quite successful [9–11]. Here we want to address the question to which extent time scale separation is crucial in order to model chaotic degrees of freedom by a noise process. Certain aspects of such a question might be answered by numerical simulations. But then one might suspect that the findings depend severely on the chosen model and are of limited relevance for real world applications. We therefore prefer to tackle the problem from the very beginning by real experiments. Our setup should be simple so that experimental conditions can be controlled

easily. We thus focus on electronic circuits. While one might suspect that certain aspects of such experiments cannot be generalized and the same limitations like in numerical simulations may apply, one has to keep in mind that several features in real experiments are universal, like the occurrence of internal dynamical and external measurement noise, the competition of these unwanted noise sources with the chaotic motion, drift of parameters, or limitations of the accessible observables and of the ensemble sizes. Thus experimental verification of stochastic modeling has higher predictive power than plain numerical analysis.

In formal terms we want to model a dynamical system, say, a chaotic differential equation $\dot{\mathbf{x}} = \mathbf{f}(\mathbf{x})$, by a suitable Langevin equation. We suppose that we can measure just a scalar time series $z(t) = g[\mathbf{x}(t)]$, e.g., a component of the state vector \mathbf{x} or a nonlinear function of the components. The essential features of the dynamics of $z(t)$ should be captured by a stochastic differential equation with Gaussian white noise source. Therefore, we need to estimate a suitable systematic part, i.e., a drift function $D_1(z)$, and a diffusion coefficient $D_2(z)$. There exists a standard recipe to obtain such quantities in terms of the first and the second moment [12]

$$\Delta t D_1(Z) = \langle [z(t + \Delta t) - z(t)] \rangle + o(\Delta t) \quad (1a)$$

$$2\Delta t D_2(Z) = \langle [z(t + \Delta t) - z(t)]^2 \rangle + o(\Delta t), \quad (1b)$$

where the averages are conditional averages with the constraint $z(t) = Z$. While for a stochastic differential equation Eqs. (1) yield the drift and diffusion in the asymptotic limit $\Delta t \rightarrow 0$ one has to observe that for the stochastic modeling of fast chaotic systems the delay Δt has to be large compared to the correlation time of the chaotic motion [13]. Apart from such a constraint Eqs. (1) have to be evaluated in the asymptotic limit of small Δt . There is of course no *a priori* guarantee whether a modeling in terms of the quantities (1) is a sufficient description, e.g.,

whether the dynamics of $z(t)$ can be described by a Markovian process or whether higher-order moments become relevant. These problems are, in particular, crucial when no pronounced time scale separation is available. Thus we have to check *a posteriori* to which extent such a stochastic description yields satisfactory results.

Experimental setup.—For our investigations we use a nonlinear autonomous electronic circuit design which was first introduced in [14]. A diagrammatic view of the circuit is shown in Fig. 1.

The device consists of an RLC circuit that is coupled to an RC element via a nonlinearity. The essential nonlinear element consists of two Zener diodes $Z_{1,2}$ (BZX85C3V3). The current-voltage characteristics of these diodes are shown in Fig. 1. Its shape is described by the expression $I_D(V_1 - V_2) = I_D(\Delta V) = \text{sgn}(\Delta V)f(|\Delta V| - V_Z)$, where $V_Z = (1.02 \pm 0.04)$ V and $f(x) = (Ax^2 + Bx^3)\Theta(x)$ denotes a third order fit with parameter values $A = (13.1 \pm 0.7)$ mA/V² and $B = (-1.59 \pm 0.15)$ mA/V³. Parallel to the oscillating part of the circuit there is a negative impedance converter (NIC), consisting of an operational amplifier (Analog Devices AD711JN), two identical feedback resistors R_1 and a resistor R_N connected to ground. This NIC acts as a linear “negative resistor” with the resistance $-R_N$ supplying the power for the circuit. The current supplied to the oscillatory part of the circuit can be controlled by variation of the adjustable resistor R . This variable resistor acts as the control parameter of the system. The other components of the circuit are fixed and the corresponding parameter values are contained in Fig. 1. We just mention that applying Kirchhoff’s rules to the circuit one easily obtains the equations of motion [15] but here we are not going to make use of such a mathematical model.

For data acquisition we used a transient recorder card (Meilhaus ME2600) to measure the voltage V_1 . This card includes also several digital output channels which were used for online variation of the control parameter by means

of several digital resistors (Xicor X9C102/4P) replacing the tunable resistor R . The fully computer controlled experiment enabled us to measure long time series for different control parameter values.

Increasing the control parameter the circuit shows the typical period doubling route to chaos. Beyond a critical control parameter value $R_c = 66$ k Ω intermittency is observed. The intermittency results from an attractor merging crisis. Below the critical control parameter R_c two symmetric attractors can be found in the phase space of the system. The initial condition determines the state which is attained in the long time asymptotics. For control parameter values above R_c a new attractor occurs, consisting of the merged precritical attractors. The symmetry of the nonlinearity is essential for the bifurcation scenario. For the particular circuit this chaos-chaos intermittency scenario can be studied in detail over a wide range of control parameter values.

The observed dynamics in the intermittency regime can be characterized by fast oscillations on the precritical attractors and a slow jump dynamics between two repelling chaotic states (see Fig. 2). The typical period of the fast oscillations is of about $T_{\text{osc}} \sim 1.5$ ms. The mean residence time τ in the two chaotic states depends on the difference between the actual and the critical control parameter, $\Delta R = R - R_c$. In our experiment we observed mean residence times from 0.1 s at $\Delta R \approx 100$ Ω to 3 ms at $\Delta R \approx 8$ k Ω . Thus our experiment allows for a dynamical range of parameter values of about 2 orders of magnitude. Close to R_c the mean residence time obeys a typical scaling law [16] $\tau \sim \Delta R^{-\gamma}$ with a critical exponent of $\gamma \sim 0.7$ [15]. Above all, a superficial inspection of the time series shows a behavior which resembles the motion of a bistable stochastic model. However, for typical parameter values of ΔR there are of about 10–100 oscillations on a chaotic saddle before a jump to the inverse image appears. Thus, time scales of the chaotic motion are not very well separated from the intermittent motion and it is far from ob-

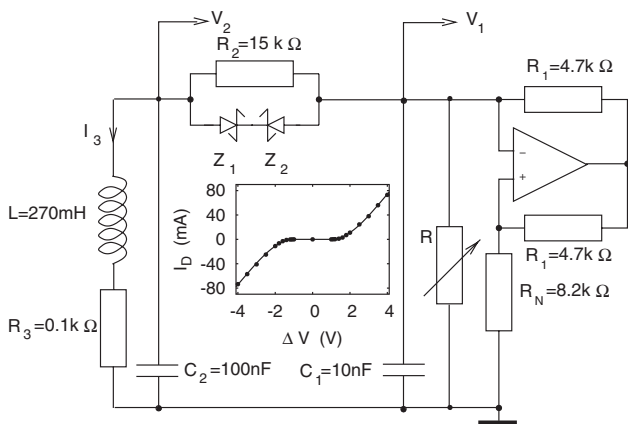


FIG. 1. Diagrammatic view of the Shinriki oscillator. Inset: experimental data (symbols) and analytical data fit (line) of the current-voltage characteristics of the two Zener diodes.

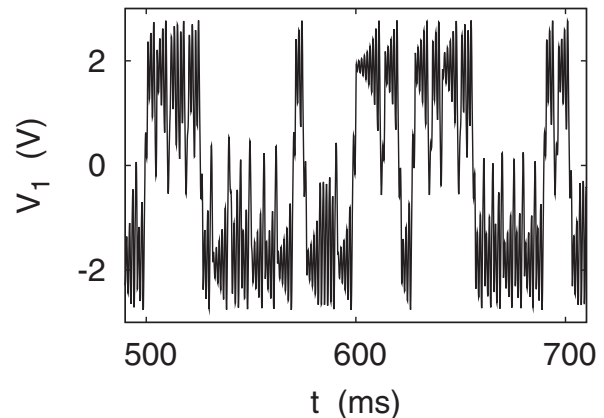


FIG. 2. Time series sample of $V_1(t)$ for $\Delta R = R - R_c = 1.1$ k Ω measured with a sampling time of 80 μ s.

vious whether a bistable stochastic model captures the essential features of the time series.

Stochastic model.—We are now going to reconstruct an effective stochastic model from experimental data of the voltage $z(t) = V_1(t)$. A time series of 6×10^5 data points with sampling time $80 \mu\text{s}$ is used to estimate the drift and the diffusion coefficient according to Eqs. (1). The basic oscillation period is of the order of $T_{\text{osc}} \sim 1.5 \text{ ms}$ at $\Delta R = 1.1 \text{ k}\Omega$ while intermittent jumps take place on a time scale of order $\tau \sim 14T_{\text{osc}}$. Evaluation of Eqs. (1) for different delays shows a plateau at an intermediate scale $\Delta t \in [2 \text{ ms}, 8 \text{ ms}]$ (cf. Fig. 3). Thus, such values can be used to estimate the parameters of our model.

Spatially resolved drift and diffusion functions have been estimated using $\Delta t = 4.5 \text{ ms}$. The conditional averages are computed on a spatial grid with step size $\Delta Z = 50 \text{ mV}$ so that approximately each data point is generated by an ensemble of size 5×10^3 . The final results are rather robust against these choices. Figure 4 shows the data obtained at $\Delta R = 1.1 \text{ k}\Omega$. The drift is dominated by a linear decay with a superimposed oscillatory structure, while the diffusion has a unimodal shape being large in center and small at the boundaries. The peak structure for $z = V_1 \in \pm[0.7 \text{ V}, 1.4 \text{ V}]$ seems to be an artifact generated by the spiky time series since no such feature shows up in the stationary distribution of the voltage (cf. inset in Fig. 4). The large scale features of drift and diffusion are stable with respect to the details of the time series analysis. Thus, despite the lack of pronounced time scale separation, the method yields reproducible drift and diffusion functions.

In order to test the accuracy of the results displayed in Fig. 4 we check whether the corresponding stochastic model predicts features of the dynamics, i.e., the mean residence time τ which can be measured independently as well. It is of course a nontrivial task to obtain mean residence times for Fokker-Planck models with nontrivial drift and diffusion coefficients. For the sake of a simple

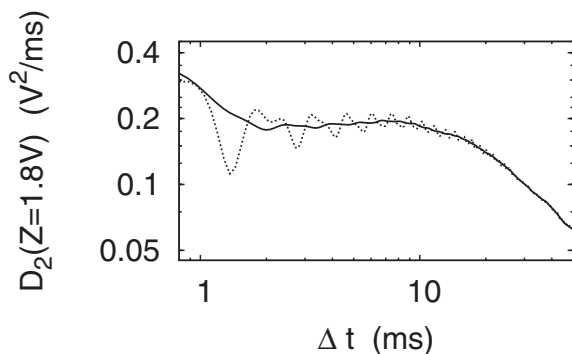


FIG. 3. Dependence of the second moment [cf. Eq. (1b)] on the time delay Δt evaluated at $Z = V_1 = 1.8 \text{ V}$. Raw data (broken line), sliding average over one period T_{osc} (solid line). Control parameter $\Delta R = 1.1 \text{ k}\Omega$. A plateau appears for $\Delta t \in [2 \text{ ms}, 8 \text{ ms}]$ while for larger values of the delay the characteristic power law decay is observed.

analytical estimate let us model the drift and diffusion coefficients just by taking into account the essential features of the graphs displayed in Fig. 4, i.e., let us approximate the drift by a linear expression, $D_1(z) = -\alpha z$ neglecting the oscillating superstructure visible in the data, and the diffusion by a parabola $D_2(z) = D(z_0^2 - z^2)$. Such an approximation seems to be quite crude as it does not take the strongly oscillating parts into account. These structures seem to be caused at least partially by the finite ensemble size since the details change slightly when time series of different lengths are considered. But no quantitative error estimates could be produced on such a basis. Thus we stay with the simple analytical choices since both analytical expressions obey the symmetry of the system, and have the tremendous advantage that the corresponding Fokker-Planck equation

$$\frac{\partial \rho(z, t)}{\partial t} = \alpha \frac{\partial z \rho(z, t)}{\partial z} + D \frac{\partial^2 (z_0^2 - z^2) \rho(z, t)}{\partial z^2} \quad (2)$$

can be solved analytically. Actually, the stationary distribution of Eq. (2) is given by $\rho_*(z) \sim (z_0^2 - z^2)^{\alpha/(2D)-1}$ showing a pronounced double peak structure for $\alpha < 2D$,

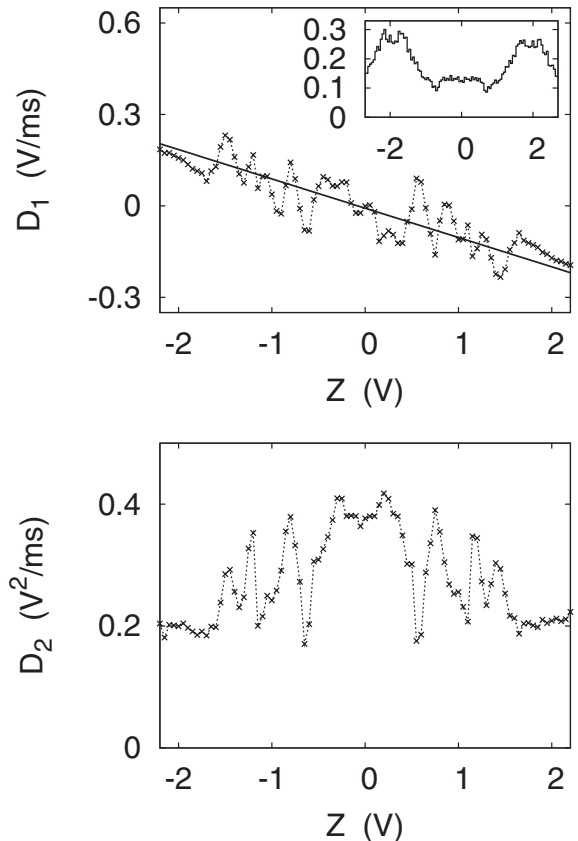


FIG. 4. Drift (top) and diffusion (bottom) evaluated for $\Delta t = 4.5 \text{ ms}$ at $\Delta R = 1.1 \text{ k}\Omega$, in dependence on the voltage $Z = V_1$ [cf. Eqs. (1)]. Conditional averages were computed with a spatial resolution $\Delta Z = 50 \text{ mV}$. The straight line indicates a least square fit in the interval $[-1.6 \text{ V}, 1.6 \text{ V}]$. Inset: distribution of V_1 as a histogram with resolution $\Delta Z = 50 \text{ mV}$.

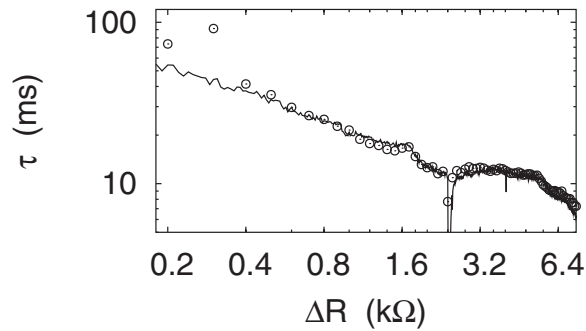


FIG. 5. Mean residence time τ in dependence on the control parameter ΔR . Line: experimental data from time series of lengths 48 s recorded with step size 10 Ω ; symbols: analytical estimate obtained from the stochastic model [cf. Eq. (2)].

while the eigenvalues of the Fokker-Planck operator which govern the time evolution read $\Lambda_n = -n\alpha - n(n-1)D$. Thus, there appears a spectral gap for $\alpha \ll D$ and the stochastic model displays a slow jump process on the time scale $\tau = 2/\alpha$.

We employ such an analytical estimate by computing the linear trend α using a least square fit in the interval $[-1.6 \text{ V}, 1.6 \text{ V}]$. Hence, we can estimate the mean residence time of the stochastic model for different values of the control parameter ΔR . Comparison with direct observations yields a remarkable coincidence (cf. Fig. 5) and the theoretical prediction is quite accurate over a wide parameter range. We therefore conclude that our stochastic model, apart from some fine structure, captures the intermittent features on the slow time scale.

Conclusion.—We have demonstrated that even without a pronounced time scale separation one may successfully model chaotic dynamics by stochastic forces. Drift and diffusion coefficients can be constructed from experimental time series. The stochastic model is able to capture the essential features of the intermittent motion, i.e., the quantitative prediction of the mean residence time over a large parameter region. The accuracy of the residence time spectrum seems to vindicate the validity of the Fokker-Planck approach at least on the relevant time scales. We made *a posteriori* checks for higher-order coefficients of the Kramers-Moyal expansion. Actually, the numerical values of the third- and fourth-order moment do not turn out to be small. An accurate test of the Markov property of the time series was not possible with the ensemble size at hand. But we estimated the time scale at which non-Markovian effects become visible to be of about 20 ms, using conditional correlation functions. Nevertheless, both shortcomings are apparently of minor importance for the modeling of the current experimental intermittent time series, as demonstrated by the results of our analysis. Above all, such good agreement may stimulate further applications of stochastic modeling in experiments.

Our simple analytical estimate for the mean residence time was certainly too crude to capture all the details of the drift and diffusion coefficients. For instance, the analytical expressions model the chaotic repellers just by fixed points. But such a simplification allows for a complete analytical solution of the stochastic model. Such solution reveals the main mechanism of the intermittent dynamics. The spatial dependence of the diffusion function, i.e., a multiplicative noise process, is crucial while the structure of a potential plays a minor role. Thus, the tunneling in such a model is dominated by diffusion. That in fact fits with the underlying chaotic dynamics which does not give rise to a bistable potential in an obvious way. Phase space dependent local Lyapunov exponents cause state dependent fluctuations.

In summary, modeling of chaotic motion by effective stochastic dynamics could have a wide range of applications even for systems without extreme time scale separation. The stochastic models may reveal features about the underlying nonlinear dynamics as well. Thus such modeling is more than just a practical tool. It might be used to uncover underlying physical mechanisms in real experiments.

*Electronic address: stemler@expl.fkp.physik.tu-darmstadt.de

†Electronic address: w.just@qmul.ac.uk

- [1] S. R. de Groot and P. Mazur, *Non-Equilibrium Thermodynamics* (North-Holland, Amsterdam, 1969).
- [2] K. Hasselmann, *Tellus* **28**, 473 (1976).
- [3] C. Beck, *J. Stat. Phys.* **79**, 875 (1995).
- [4] D. Givon, R. Kupferman, and A. Stuart, *Nonlinearity* **17**, R55 (2004).
- [5] C. Robinson, *Dynamical Systems: Stability, Symbolic Dynamics, and Chaos* (CRC Press, Boca Raton, 1995).
- [6] R. Friedrich and J. Peinke, *Phys. Rev. Lett.* **78**, 863 (1997).
- [7] R. Friedrich, J. Peinke, and C. Renner, *Phys. Rev. Lett.* **84**, 5224 (2000).
- [8] A. Majda, I. Timofeyev, and E. Vanden-Eijnden, *Nonlinearity* **19**, 769 (2006).
- [9] F. Jülicher, A. Ajdari, and J. Prost, *Rev. Mod. Phys.* **69**, 1269 (1997).
- [10] A. Neiman and D. F. Russell, *Phys. Rev. Lett.* **86**, 3443 (2001).
- [11] P. Reimann, *Phys. Rep.* **361**, 57 (2002).
- [12] H. Risken, *The Fokker-Planck Equation: Methods of Solution and Applications* (Springer, New York, 1989).
- [13] H. Kantz, W. Just, N. Baba, K. Gelfert, and A. Riegert, *Physica (Amsterdam)* **187D**, 200 (2004).
- [14] M. Shinriki, M. Yamamoto, and S. Mori, *Proc. IEEE* **69**, 394 (1981).
- [15] J. P. Werner, T. Stemler, and H. Benner, *Crisis and Stochastic Resonance in Shinriki's Circuit*, TU-Darmstadt report, 2006.
- [16] C. Grebogi, E. Ott, and J. A. Yorke, *Physica (Amsterdam)* **7D**, 181 (1983).